POD Model reduction of parametric PDEs

David Ryckelynck

Centre des Matériaux, Mines ParisTech
David.Ryckelynck@mines-paristech.fr

The COSIMOR scientific network

The Co-Simulation and Model Order-Reduction newtwork is supported by the DFG.

Felix Fritzen, Bernard Haasdonk, Varvara Kouznetsova, Annika Radermacher, David Ryckelynck , Judith Schneider, Sebastian Schöps

4th International Workshop on Order-Reduction Methods for application to mechanics of materials
EUROMECH 2018,
Aug 28th - Wed, Aug 31st, 2018, Bad Herrenalb, Germany

Usually solutions of partial differential equations(DPEs) are sought as a field of a spatial variable

Parameters are selected to set partial differential equations (PDEs), but solutions are denoted by:

$$\mathbf{u}(\mathbf{x}), \quad \mathbf{x} \in \Omega$$

Often, discussions about parameters are weak, although more and more numerical simulations are performed in order to understand the effect of parameters on solutions.

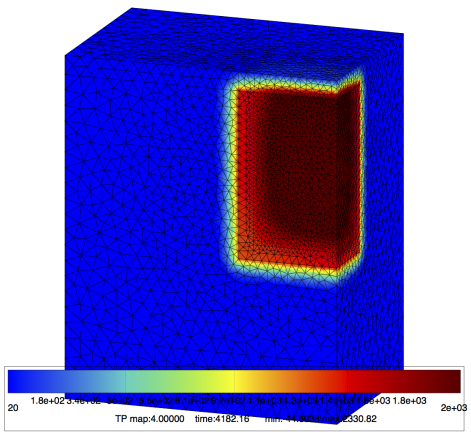

Prediction of a temperature field for casting simulation.

PDE solutions are more than fields!

Outline

1. Images and tensors
2. Tensor format of PDE solutions and matricization
3. Singular value decomposition (SVD)
4. PDE solution by using the finite element method
5. The setting of the Reduced equations
6. Numerical example

Outline

1. Images and tensors
2. Tensor format of PDE solutions and matricization
3. Singular value decomposition (SVD)
4. PDE solution by using the finite element method
5. The setting of the Reduced equations
6. Numerical example

Empirical Orthogonal Functions and Statistical Weather Prediction

Data mining of 64 pressure sensors over the USA.

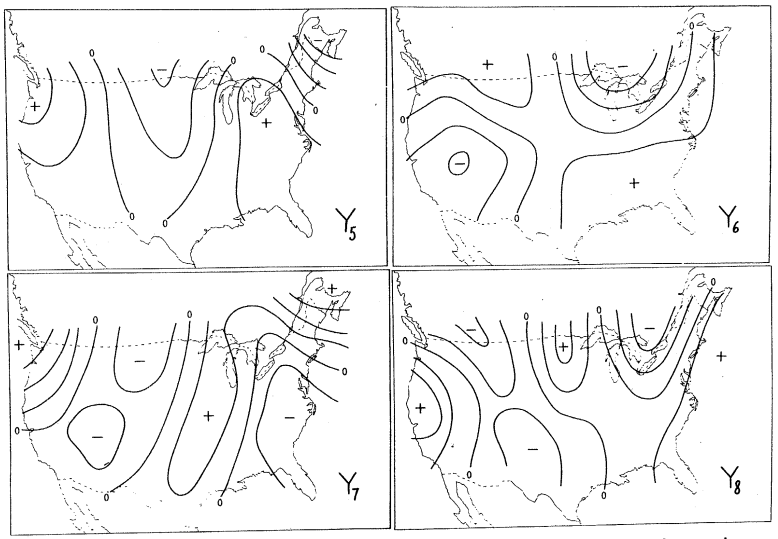

Fig. 2. Maps of the empirical orthogonal functions of space, $Y_1, \ldots, Y_8$. Isopleths are drawn at intervals of 0.1 unit. The zero isopleths are labeled. The units are chosen so that the sum of the squares of a function, at the 64 stations is 1.

Integration of dynamic equations by using empirical modes was first suggested in 1956[1].

$$\mathbf{p} = \mathbf{V}\,\boldsymbol{\gamma},\ \mathbf{V} \in \mathbb{R}^{64\times 8}$$

[1] E. N. Lorenz, Empirical Orthogonal Functions and Statistical Weather Prediction, Sc. Report, Statistical Forecasting Project, MIT, 1956

Images and 2-order tensors

Greyscale digital images can be considered as matrices, or 2-order tensors.

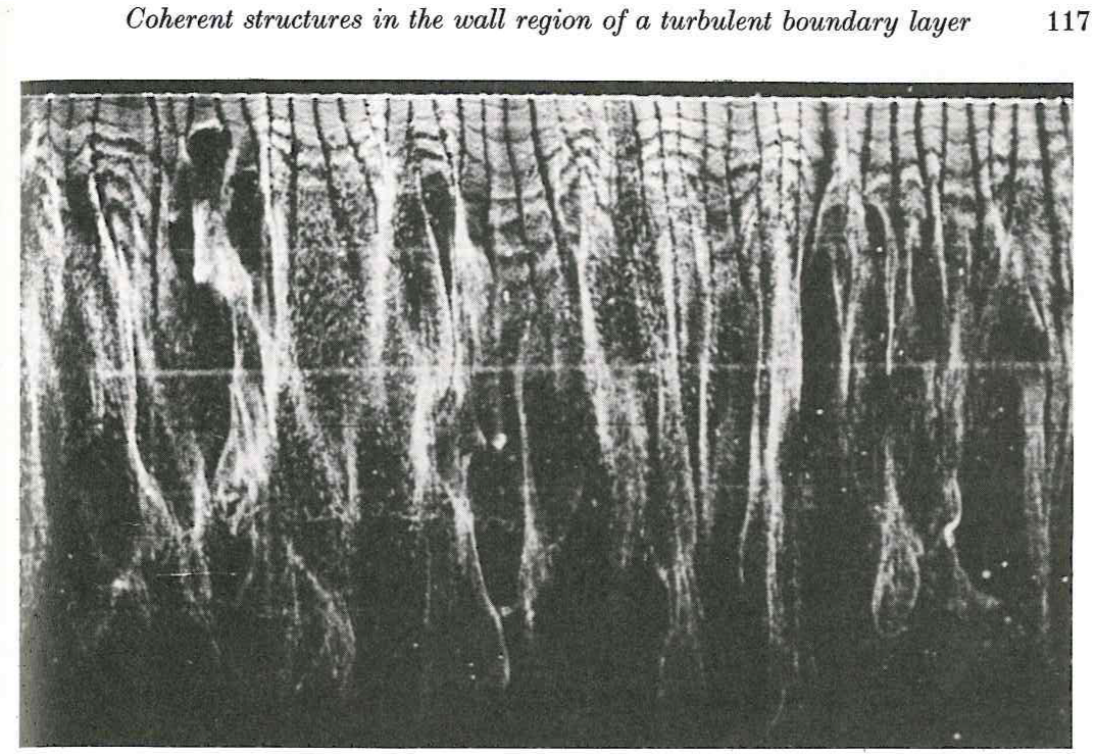

FIGURE 1. Bubble-wire visualization of the turbulent boundary layer at $x_2^+ = 6.6$. A single frame from the movie taken by S. Kline at Stanford University (see Kline *et al.* 1967) and kindly provided by S. Kline.

In Aubry, Holmes, Lumley, Stone (1988)[2]

$$\mathbf{Q} \in \mathbb{R}^{N_y \times N_x} \rightarrow \mathbf{V} \in \mathbb{R}^{N_y \times N}, \; N < N_x$$

First solution of a PDE by using empirical modes.

[2] N. Aubry, P. Holmes, J.L. Lumley, E. Stone, The dynamics of coherent structures in the wall region of a turbulent boundary layer, J. Fluid Mech., 192, pp. 115-173 (1988)

Karhunen–Loève procedure for gappy data[3]

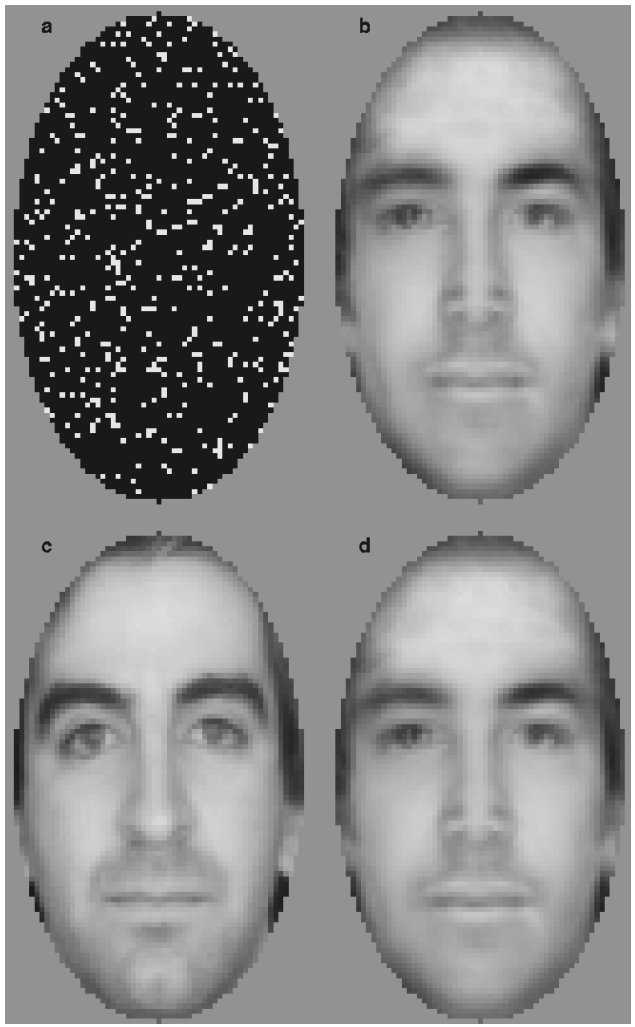

$$\mathbf{Q} \in \mathbb{R}^{(N_x N_y) \times m}, \quad \mathbf{V} \in \mathbb{R}^{(N_x N_y) \times N}$$

Reconstruction of a face, not in the original ensemble from a 10% mask. The reconstructed face, (b), was determined with 50 empirical eigenfunctions and only the white pixels shown in (a). The original face is shown in (c), and a projection (with all the pixels) of the face onto 50 empirical eigenfunctions is shown in (d). The masked image is the vector **Zf** (**Z** is a truncated identity matrix):

$$\boldsymbol{\gamma} = \arg\min_{\boldsymbol{\gamma}^\star} \|(\mathbf{Zf}) - \mathbf{ZV}\boldsymbol{\gamma}^\star\|_2$$

$$\Rightarrow \boldsymbol{\gamma} = \left(\mathbf{V}^T\mathbf{Z}^T\mathbf{ZV}\right)^{-1}\mathbf{V}^T\mathbf{Z}^T\left(\mathbf{Zf}\right)$$

The reconstructed image reads:

$$\mathbf{f}_{Gappy} = \mathbf{V}\left(\mathbf{V}^T\mathbf{Z}^T\mathbf{ZV}\right)^{-1}\mathbf{V}^T\mathbf{Z}^T\left(\mathbf{Zf}\right)$$

[3] Karhunen-Loève procedure for gappy data, R. Everson, L. Sirovich, J. Opt. Soc. Am. A, Vol. 12, 8 (1995)

More recent results on tensor completion[4]


The left figure contains 80% missing entries shown as white pixels and the right figure shows its reconstruction using the low rank approximation.

Color images are at least 3 order tensors $u(i, j, k)$, (i,j) is related to the pixel location and k to the color (k = R,G,B for instance).

[4] Tensor Completion for Estimating Missing Values in Visual Data, Ji Liu, Przemyslaw Musialski, Peter Wonka, and Jieping Ye, (2012)

Outline

1. Images and tensors
2. Tensor format of PDE solutions and matricization
3. Singular value decomposition (SVD)
4. PDE solution by using the finite element method
5. The setting of the Reduced equations
6. Numerical example

Tensor format of PDE solutions

For model reduction, we consider a set of fields over $\Omega \times [0, T]$ for time dependent problems, or over $\Omega \times \mathcal{D}$ for solutions of parametric differential equations, where $\mathcal{D}$ is the parameter space.

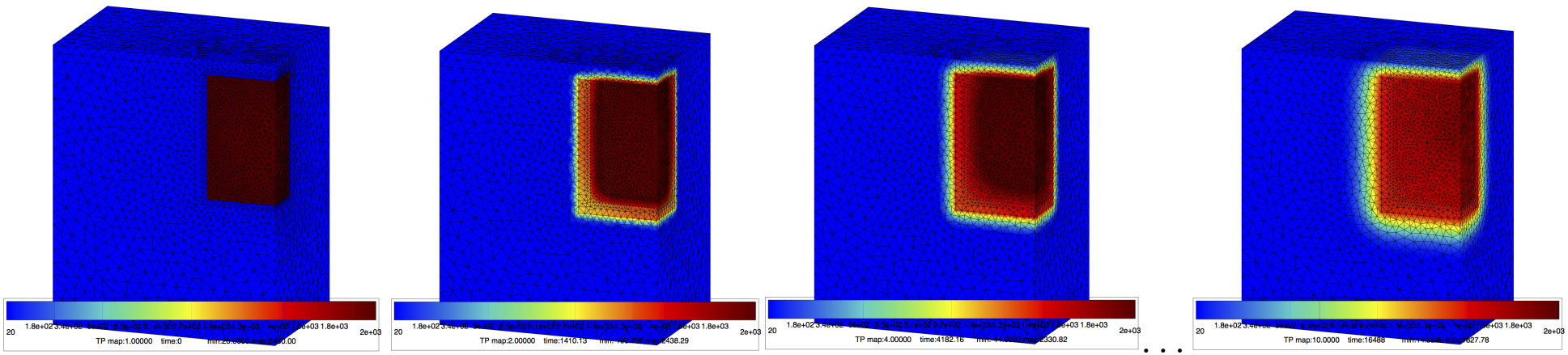

Temperature fields during a transient thermal simulation.

Tensor format of PDEs solutions

Solutions of balance equations are tensors when considering the entire domain of variation of all variables:

$$\mathbf{u}(\mathbf{x}, t) \in \mathcal{V} \otimes \mathcal{C}, \quad (\mathbf{x}, t) \in \Omega \times [0, T]$$

One can define a multilinear application by introducing integrals:

$$\mathbf{v}(\mathbf{x}) \in \mathcal{V}^\star, \quad g(t) \in \mathcal{C}^\star \quad \rightarrow \quad T_u(\mathbf{v}, g) := \int_\Omega \int_0^T \mathbf{u}(\mathbf{x}, t)\, \mathbf{v}(\mathbf{x})\, g(t)\, \omega\, dx\, dt \quad \in \mathbb{R}$$

Here, $\mathbf{u}$ has two variables. It is a second order tensor.

Here $\mathcal{V}$ and $\mathcal{C}$ are vector spaces for space and time functions respectively. The dual vector spaces for space functions and time function are:

$$\mathbf{v}(\mathbf{x}) \in \mathcal{V}^\star, \quad g(t) \in \mathcal{C}^\star$$

High dimensional tensor

When considering the solution as a function of more than 2 variables $(\mathbf{x}, \mu_1, \ldots, \mu_{D-1})$, $\mu_i \in [\mu_i^{min},\ \mu_i^{max}]$, we obtain a tensor of order D ($D > 2$):

$$\mathbf{v}(\mathbf{x}) \in \mathcal{V}^\star,\ g_1(\mu_1) \in \mathcal{C}_1^\star, \ldots,\ g_{D-1}(\mu_{D-1}) \in \mathcal{C}_{D-1}^\star \quad \rightarrow \quad T_u(\mathbf{v}, g_1, \ldots, g_{D-1}) \quad \in \mathbb{R}$$

$$T_u := \int_\Omega \int_{\mu^{1\,min}}^{\mu^{1\,max}} \ldots \int_{\mu^{D-1\,min}}^{\mu^{D-1\,max}} \mathbf{u}(\mathbf{x}, \mu^1, \ldots, \mu^{D-1})\mathbf{v}(\mathbf{x}) g_1(\mu^1) \ldots g_{D-1}(\mu^{D-1}) \omega\, dx\, d\mu^1 \ldots d\mu^{D-1}$$

Here the solution is defined over the domain:

$$\Omega \times [\mu^{min\,1},\ \mu^{max\,1}] \times \ldots \times [\mu^{min\,D-1},\ \mu^{max\,D-1}]$$

Tensors in finite element setting

Let's introduce finite element shape functions $(\varphi_1, \ldots, \varphi_{\mathcal{N}})$ defined over the domain $\Omega \subset \mathbb{R}^d$, and a time discretization $\{t_1, \ldots, t_m\}$.

$$\mathbf{u}_h(\mathbf{x}, t_j) := \sum_{i=1}^{\mathcal{N}} \varphi_i(\mathbf{x})\, q_i(t_j), \quad \mathcal{V}_h := \text{span}(\varphi_1, \ldots, \varphi_{\mathcal{N}}) \subset \mathcal{V}$$

A numerical simulation gives access to a matrix of snapshots (second order tensor):

$$\mathbf{Q} \in \mathbb{R}^{\mathcal{N} \times m}, \quad Q_{ij} = q_i(t_j)$$

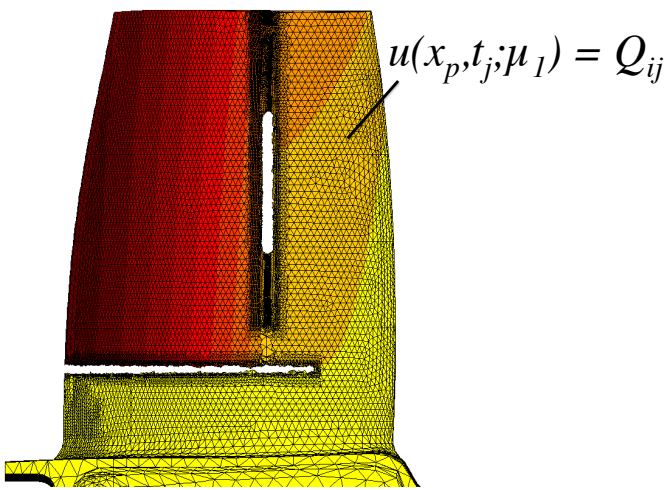

$$\varphi_i(\mathbf{x}) = \varphi_p^{1D}(\mathbf{x})\, \mathbf{e}_k$$
$$i = (p-1)\, d + k$$
$$k = 1, \ldots, d$$
$$p = 1, \ldots, \mathcal{N}_o$$

Example of snapshot extracted from a mechanical simulation of a modified turbine blade.

Modal unfolding of order-D tensors

To unfold a tensor (FR: déployer un tenseur) is to arrange its entries in a matrix.

In the first modal unfolding, all variables of $\mathbf{u}$, except the first one, are grouped in a single multidimensional variable $\boldsymbol{\mu} = (\mu_1, \ldots, \mu_{D-1})$.

$$\mathbf{u}(\mathbf{x}_i, \mu_j^1, \ldots, \mu_j^{D-1}) = \mathbf{u}_{(1)}(\mathbf{x}_i, \boldsymbol{\mu}_j),\ \mathbf{x}_i \in \Omega,\ \boldsymbol{\mu}_j \in \mathcal{P} = Q_{(1)ij}$$

Here, each column of $\mathbf{Q}_{(1)}$ contains all the nodal values of the field related to a given vector of parameters.

Modal unfolding of order-D tensors

To unfold a tensor (FR: déployer un tenseur) is to arrange its entries in a matrix.

In the first modal unfolding, all variables of $\mathbf{u}$, except the first one, are grouped in a single multidimensional variable $\boldsymbol{\mu} = (\mu_1, \ldots, \mu_{D-1})$.

$$\mathbf{u}(\mathbf{x}_i, \mu_j^1, \ldots, \mu_j^{D-1}) = \mathbf{u}_{(1)}(\mathbf{x}_i, \boldsymbol{\mu}_j),\ \mathbf{x}_i \in \Omega,\ \boldsymbol{\mu}_j \in \mathcal{P} = Q_{(1)ij}$$

Here, each column of $\mathbf{Q}_{(1)}$ contains all the nodal values of the field related to a given vector of parameters.

Curse of dimension : If a regular grid of 10 steps per parameter μ^k is introduced for the discretization of $\mathcal{D}$, then $\mathbf{Q}_{(1)}$ has $\mathcal{N}$ rows and 10^{D-1} columns!

Remarks:

- In most cases, $\mathbf{Q}_{(1)}$ is not sparse.
- The TT-cross approximation proposed by Y. Oseledets and E. Tyrtyshnikov in 2010, starts by a decomposition of $\mathbf{Q}_{(1)}$.

Outline

1. Images and tensors
2. Tensor format of PDE solutions and matricization
3. Singular value decomposition (SVD)
4. PDE solution by using the finite element method
5. The setting of the Reduced equations
6. Numerical example

Singular value decomposition or Principal Component Analysis

The thin SVD: Let $\overline{\mathbf{Q}} \in \mathbb{R}^{\mathcal{N} \times \overline{m}}$ be the matrix containing all the PDE solutions. There exist orthogonal matrices

$$\overline{\mathbf{V}} = [\mathbf{v}_1 \dots \mathbf{v}_m] \in \mathbb{R}^{\mathcal{N} \times m}, \quad \overline{\mathbf{V}}^T \overline{\mathbf{V}} = \mathbf{I}_m$$

$$\overline{\mathbf{W}} = [\mathbf{w}_1 \dots \mathbf{w}_m] \in \mathbb{R}^{m \times m}, \quad \overline{\mathbf{W}}^T \overline{\mathbf{W}} = \mathbf{I}_m$$

and a diagonal matrix containing the singular values of $\overline{\mathbf{Q}}$

$$\overline{\mathbf{S}} = \text{diag}(\sigma_1, \dots, \sigma_m), \text{ where } \sigma_1 \geq \dots \geq \sigma_m \geq 0$$

such that:

$$\overline{\mathbf{Q}} = \overline{\mathbf{V}}\,\overline{\mathbf{S}}\,\overline{\mathbf{W}}^T$$

The rank is obtained by:

$$\text{rank}(\overline{\mathbf{Q}}) = \arg \max_{k,\, \sigma_k > 0} k \quad \leq \min(\mathcal{N}, \overline{m})$$

Property: if $\text{rank}(\overline{\mathbf{Q}}) \leq \mathcal{N}$ then $\overline{\mathbf{V}}[:, 1, \dots, \text{rank}(\overline{\mathbf{Q}})]$ is a reduced basis.

A posteriori model reduction

In most cases, it is not possible to have access to all possible solutions: $\overline{\mathbf{Q}} \in \mathbb{R}^{\mathcal{N} \times \overline{m}}$. In *a posteriori* model reduction approach, simulations are ran before computing empirical modes.

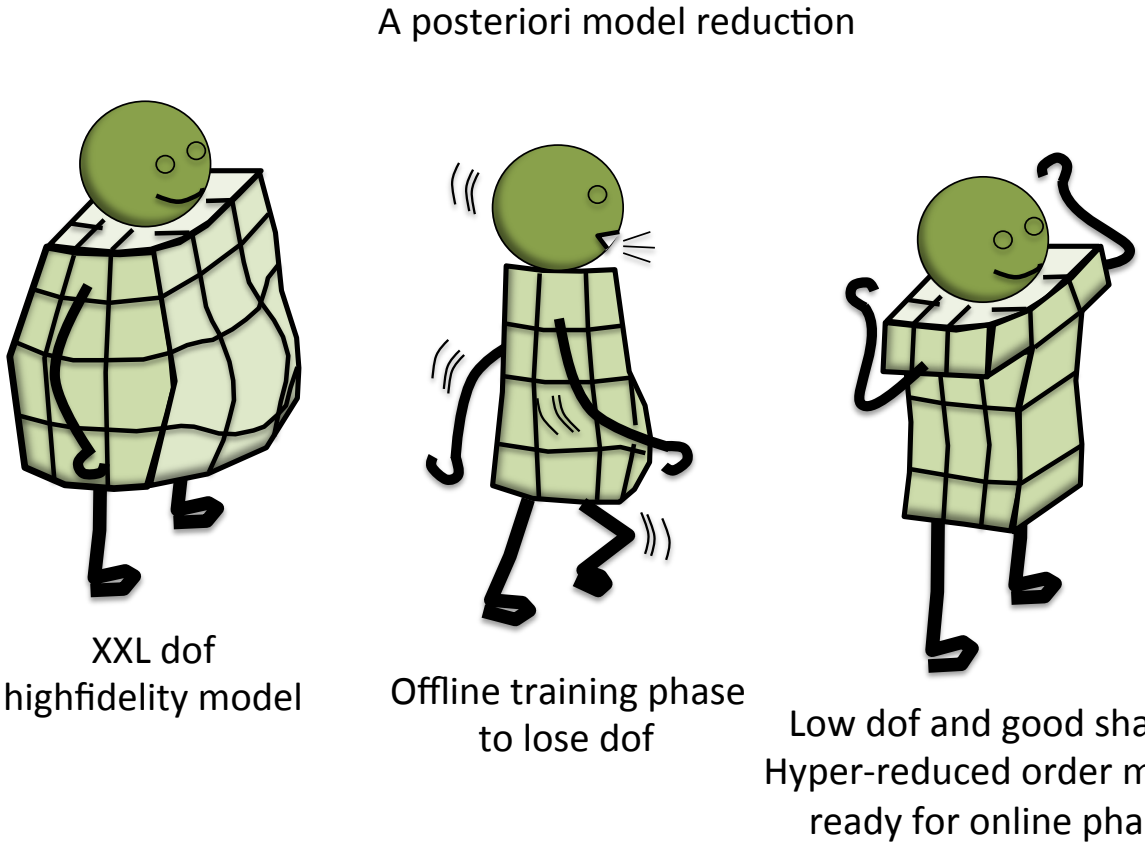

This approach is very convenient for the reduction of nonlinear PDEs, because there is no assumption about the PDE when collecting data.

A random sampling of $\mathcal{D}$ or $[0, T]$ is introduced to collect data.

$$\mathbf{Q} = [\overline{\mathbf{q}}_j]_{j \in \Sigma_{train}} \in \mathbb{R}^{\mathcal{N} \times m},\ m = \text{Card}(\Sigma_{train}),\ m \leq \mathcal{N}$$

Truncated SVD

$$\mathbf{V} = [\mathbf{v}_1 \dots \mathbf{v}_N] \in \mathbb{R}^{\mathcal{N} \times N},\ N \leq \text{rank}(\mathbf{Q})$$

$$\mathbf{W} = [\mathbf{w}_1 \dots \mathbf{w}_N] \in \mathbb{R}^{m \times N}$$

$$\mathbf{S} = \text{diag}(\sigma_1, \dots, \sigma_N)$$

such that

$$\mathbf{Q} = \mathbf{V}\,\mathbf{S}\,\mathbf{W}^T + \mathbf{R}, \quad \|\mathbf{R}\|_F^2 = \sum_{k=N+1}^{\text{rank}(\mathbf{Q})} \sigma_k^2, \quad \|\mathbf{R}\|_2 = \sigma_{N+1}$$

and $\mathbf{S}^{-1}$ exists.

Frobenius norm : $\|\mathbf{R}\|_F^2 = \sum_i \sum_j r_{ij}^2$
Matrix 2-norm : $\|\mathbf{R}\|_2^2 = \lambda_{max}(\mathbf{R}^T\,\mathbf{R})$

The Eckhart-Young theorem [5]

The SVD decomposition is optimal: it is the best rank-N decomposition of $\mathbf{Q}$,

$$\mathbf{Q}^{(N)} = \sum_{i=1}^{N} \sigma_i \, \mathbf{v}_i \, \mathbf{w}_i^T = \mathbf{V} \, \mathbf{S} \, \mathbf{W}^T,$$

$$\min_{\text{rank}(\mathbf{B})=N} \|\mathbf{Q} - \mathbf{B}\|_2 = \|\mathbf{Q} - \mathbf{Q}^{(N)}\|_2 = \sigma_{N+1}$$

where $\| \cdot \|_2$ is the matrix 2-norm.

[5] Matrix Computations, 4th ed., G. H. Golub, C.F. Van Loan, The Johns Hopkins University Press, Baltimore, (2013)

Snapshot POD[6]

$(\sigma_k^2)_{k=1}^m$ are the eigenvalues of the following correlation matrix, $\mathbf{Q}^T\,\mathbf{Q}$:

$$\mathbf{Q}^T\,\mathbf{Q}\,\mathbf{w}_k = \mathbf{w}_k\,\sigma_k^2, \quad k = 1, \ldots m$$

or

$$\mathbf{Q}^T\,\mathbf{Q}\,\mathbf{W} = \mathbf{W}\,\mathbf{S}^2$$

and

$$\mathbf{V} = \mathbf{Q}\,\mathbf{W}\,\mathbf{S}^{-1}$$

Usually, we assume that $\mathbf{V}$ is a good candidate for the approximation of the subspace spanned by the columns of $\overline{\mathbf{Q}}$.

[6] Turbulence and the dynamics of coherent structures, parts I-III., L. Sirovich, Quarterly of Applied Mathematics, XLV:561-590, (1987)

Proper Orthogonal Decomposition with respect to L^2 norm

POD empirical modes are fields defined over Ω.

Proper orthogonal modes ψ_k are solutions of:

$$\min_{\psi_k^\star,\ \|\psi_k^\star\|_{L^2}=1} \sum_{j=1}^{m} \|\mathbf{u}(\cdot,j) - \sum_{k=1}^{N} \psi_k^\star \ < \psi_k^\star, \mathbf{u}(\cdot,j) > \|^2_{L^2(\Omega)}$$

$$< \mathbf{u}, \mathbf{v} >= \int_\Omega \mathbf{u}\,\mathbf{v}\, d\Omega, \qquad \|\mathbf{u}\|^2_{L^2(\Omega)} =< \mathbf{u}, \mathbf{u} >$$

Property: POD modes are orthogonal

$$< \psi_k, \psi_p >= \delta_{kp}$$

Proper Orthogonal Decomposition with respect to L^2 norm

POD empirical modes are fields defined over Ω.

Proper orthogonal modes ψ_k are solutions of:

$$\min_{\psi_k^\star,\ \|\psi_k^\star\|_{L^2}=1} \sum_{j=1}^{m} \|\mathbf{u}(\cdot,j) - \sum_{k=1}^{N} \psi_k^\star \ < \psi_k^\star, \mathbf{u}(\cdot,j) > \|^2_{L^2(\Omega)}$$

$$< \mathbf{u}, \mathbf{v} >= \int_\Omega \mathbf{u}\,\mathbf{v}\, d\Omega, \qquad \|\mathbf{u}\|^2_{L^2(\Omega)} =< \mathbf{u}, \mathbf{u} >$$

Property: POD modes are orthogonal

$$< \psi_k, \psi_p >= \delta_{kp}$$

SVD modes of $\widetilde{\mathbf{Q}} = \mathbf{L}^T\,\mathbf{Q}$ gives access to POD modes, if $\mathbf{M} = \mathbf{L}\mathbf{L}^T$ according to the Cholesky decomposition, with $m_{ij} = \int_\Omega \varphi_i \varphi_j\, d\Omega$, such that

$$\psi_k = \sum_{i=1}^{\mathcal{N}} \varphi_i\, v_{ik}^{\psi}, \qquad \mathbf{V}^{\psi} = \mathbf{L}^{-T}\mathbf{V}$$

More details in the work of S. Volkwein.

Proof

Let's consider

$$\mathbf{v}(\cdot,j) = \sum_{i=1}^{\mathcal{N}} \varphi_i \, p_{ij}, \; \mathbf{u}(\cdot,j) = \sum_{i=1}^{\mathcal{N}} \varphi_i \, q_{ij} \; \Rightarrow < \mathbf{v}(\cdot,j), \mathbf{u}(\cdot,j) >= \mathbf{p}_j^T \mathbf{M} \mathbf{q}_j = (\mathbf{P}^T \mathbf{M} \mathbf{Q})_{jj}$$

Let's consider

$$\mathbf{M} = \mathbf{L}\mathbf{L}^T, \quad \widetilde{\mathbf{Q}} = \mathbf{L}^T \, \mathbf{Q}, \quad \psi_k^\star = \sum_{i=1}^{\mathcal{N}} \varphi_i \, v_{ik}^{\psi\star}, \quad \mathbf{V}^{\psi\star} = \mathbf{L}^{-T} \mathbf{V}^\star, \; \mathbf{V}^{\star T} \mathbf{V}^\star = \mathbf{I}_N$$

Proof

Let's consider

$$\mathbf{v}(\cdot,j) = \sum_{i=1}^{\mathcal{N}} \varphi_i \, p_{ij}, \; \mathbf{u}(\cdot,j) = \sum_{i=1}^{\mathcal{N}} \varphi_i \, q_{ij} \; \Rightarrow < \mathbf{v}(\cdot,j), \mathbf{u}(\cdot,j) >= \mathbf{p}_j^T \mathbf{M} \mathbf{q}_j = (\mathbf{P}^T \mathbf{M} \mathbf{Q})_{jj}$$

Let's consider

$$\mathbf{M} = \mathbf{L}\mathbf{L}^T, \quad \widetilde{\mathbf{Q}} = \mathbf{L}^T \, \mathbf{Q}, \quad \boldsymbol{\psi}_k^\star = \sum_{i=1}^{\mathcal{N}} \varphi_i \, v_{ik}^{\psi\star}, \quad \mathbf{V}^{\psi\star} = \mathbf{L}^{-T} \mathbf{V}^\star, \; \mathbf{V}^{\star T} \mathbf{V}^\star = \mathbf{I}_N$$

Then

$$\text{rank}(\mathbf{V}^\star \, (\mathbf{V}^{\star T} \, \widetilde{\mathbf{Q}})) \leq N \text{ (we assume, } = N), \quad \text{and}$$

$$\sum_{j=1}^{m} \|\mathbf{u}(\cdot,j) - \sum_{k=1}^{N} \boldsymbol{\psi}_k^\star \; < \boldsymbol{\psi}_k^\star, \mathbf{u}(\cdot,j) > \|^2_{L^2(\Omega)} = \text{Tr}[(\mathbf{Q} - \mathbf{V}^{\psi\star} \, (\mathbf{V}^{\psi\star T} \, \mathbf{M}\mathbf{Q}))^T \, \mathbf{M} (\mathbf{Q} - \mathbf{V}^{\psi\star} \, (\mathbf{V}^{\psi\star T} \, \mathbf{M}\mathbf{Q}))]$$

$$= \text{Tr}[(\widetilde{\mathbf{Q}} - \mathbf{V}^\star \, (\mathbf{V}^{\star T} \, \widetilde{\mathbf{Q}}))^T \, (\widetilde{\mathbf{Q}} - \mathbf{V}^\star \, (\mathbf{V}^{\star T} \, \widetilde{\mathbf{Q}}))]$$

whose minimum is the SVD of $\widetilde{\mathbf{Q}}$.

$$\mathbf{V}^T \mathbf{V} = \mathbf{I} \; \Rightarrow \; \mathbf{V}^{\psi T} \, \mathbf{L} \, \mathbf{L}^T \, \mathbf{V}^\psi = \mathbf{I} \; \Rightarrow < \boldsymbol{\psi}_k, \boldsymbol{\psi}_p >= \delta_{kp}$$

Fundamental assumption

All data are related to the same discretization of Ω: a unique mesh.

The mesh is assumed to be convenient for accurate predictions related to all parameters and all time instants!

In most cases, mesh adaptation is not the purpose of model reduction methods.

Outline

1. Images and tensors
2. Tensor format of PDE solutions and matricization
3. Singular value decomposition (SVD)
4. PDE solution by using the finite element method
5. The setting of the Reduced equations
6. Numerical example

The Finite Element (FE) method

Let's consider the following balance equation:

$$\mathbf{u} \in \mathbf{u}^d + \mathcal{V}, \quad \mathcal{L}(\mathbf{u}) = 0 \; \forall \mathbf{x} \in \Omega, \quad (\text{e.g. } \mathcal{L} = \rho \, \ddot{\mathbf{u}} - \mathbf{div}(\mathbf{C} \, \boldsymbol{\varepsilon}(\mathbf{u})) \;)$$

what ever the material is, and what ever the boundary conditions are, the weak form of the FE equations reads:

$$\mathbf{u} \in \mathbf{u}^d + \mathcal{V}_h, \quad \mathcal{V}_h = \text{span}(\boldsymbol{\varphi}_i)_{i=1}^{\mathcal{N}} \subset \mathcal{V}, \quad \int_\Omega \mathcal{L}(\mathbf{u}) \, \mathbf{v}^* \, d\Omega = 0 \quad \forall \mathbf{v}^* \in \mathcal{V}_h$$

$$\mathbf{u}(\mathbf{x}, t) = \mathbf{u}^d + \sum_{i=1}^{\mathcal{N}} \boldsymbol{\varphi}_i(\mathbf{x}) \, q_i(t)$$

This is a full order model (FOM).

Cea's lemma

Let V be a real Hilbert space with the norm $\|\cdot\|$.

In case of elliptic problems, let's introduce a bilinear form:

$$a(\mathbf{v},\mathbf{w}) = \int_\Omega \mathbf{w}\,(\mathcal{L}(\mathbf{v}) - \mathcal{L}(0))\,dx \;\in \mathbb{R}$$

with the property, $\exists \gamma > 0,\ \alpha > 0$ such that:

- $|a(\mathbf{v},\mathbf{w})| \leq \gamma \|\mathbf{v}\|\ \|\mathbf{w}\|\ \forall\ \mathbf{v},\ \mathbf{w}$ (Continuity)
- $a(\mathbf{v},\mathbf{v}) \geq \alpha\ \|\mathbf{v}\|^2$ (Coercivity)

and a linear form:

$$b(\mathbf{w}) = \int_\Omega \mathbf{w}\,\mathcal{L}(0)\,dx \;\in \mathbb{R}$$

Let's denote by $\mathbf{u}_h$ the unique (Lax-Milgram theorem) FE approximation of the unique exact solution $\mathbf{u}$:

$$\mathbf{u}_h \in \mathcal{V}_h \subset \mathcal{V},\ a(\mathbf{u}_h,\mathbf{w}) = b(\mathbf{w})\ \forall \mathbf{w} \in \mathcal{V}_h$$

Cea's lemma states:

$$\|\mathbf{u} - \mathbf{u}_h\| \leq \frac{\gamma}{\alpha} \min_{\mathbf{v}\in\mathcal{V}_h} \|\mathbf{u} - \mathbf{v}\|$$

The lower the projection error on $\mathcal{V}_h$ of $\mathbf{u}$, the better the solution $\mathbf{u}_h$.

This lemma is valid for all subspaces of $\mathcal{V}$, especially for $\mathcal{V}_{ROM} \subset \mathcal{V}_h$.

Usual offline procedure when using the Proper Orthogonal Decomposition (POD)

During the design of the experimental set-up: the numerical results of preliminary FE solutions are considered as data for the snapshot POD [Sirovich 1987].

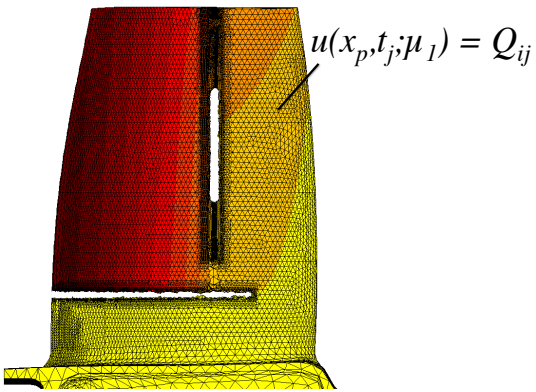

$$\forall \mathbf{x} \in \Omega$$

$$\mathbf{u}(\mathbf{x}, t_j; \boldsymbol{\mu}_1) = \mathbf{u}_o + \sum_{i=1}^{\mathcal{N}} \varphi_i(\mathbf{x})\, Q_{ij}$$

$$\mathcal{V}_h = \text{span}(\varphi_1, \ldots, \varphi_{\mathcal{N}})$$

These data are the inputs of a singular value decomposition (SVD).

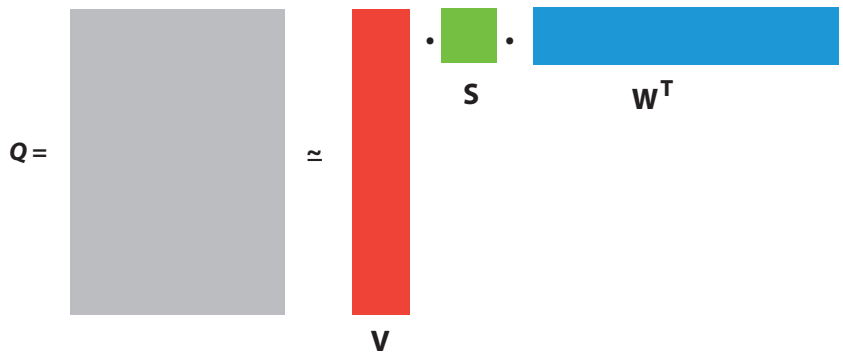

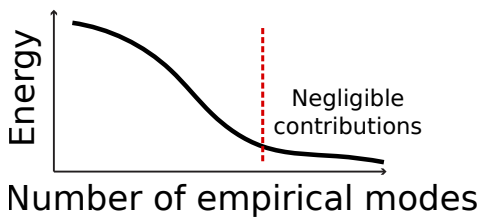

$$\mathbf{u}_{ROM}(\mathbf{x}, t; \boldsymbol{\mu}) = \sum_{k=1}^{N} \psi_k(\mathbf{x})\, \gamma_k(t; \boldsymbol{\mu}), \quad \psi_k(\mathbf{x}) = \sum_{i=1}^{\mathcal{N}} \varphi_i(\mathbf{x})\, V_{ik}, \; N << \mathcal{N}$$

Numerical example, POD modes (Z-set code)

We have performed the simulation of 5 load cycles. The POD Reduced Basis has 6 empirical modes. Additional modes can be obtained by the DEPOD.

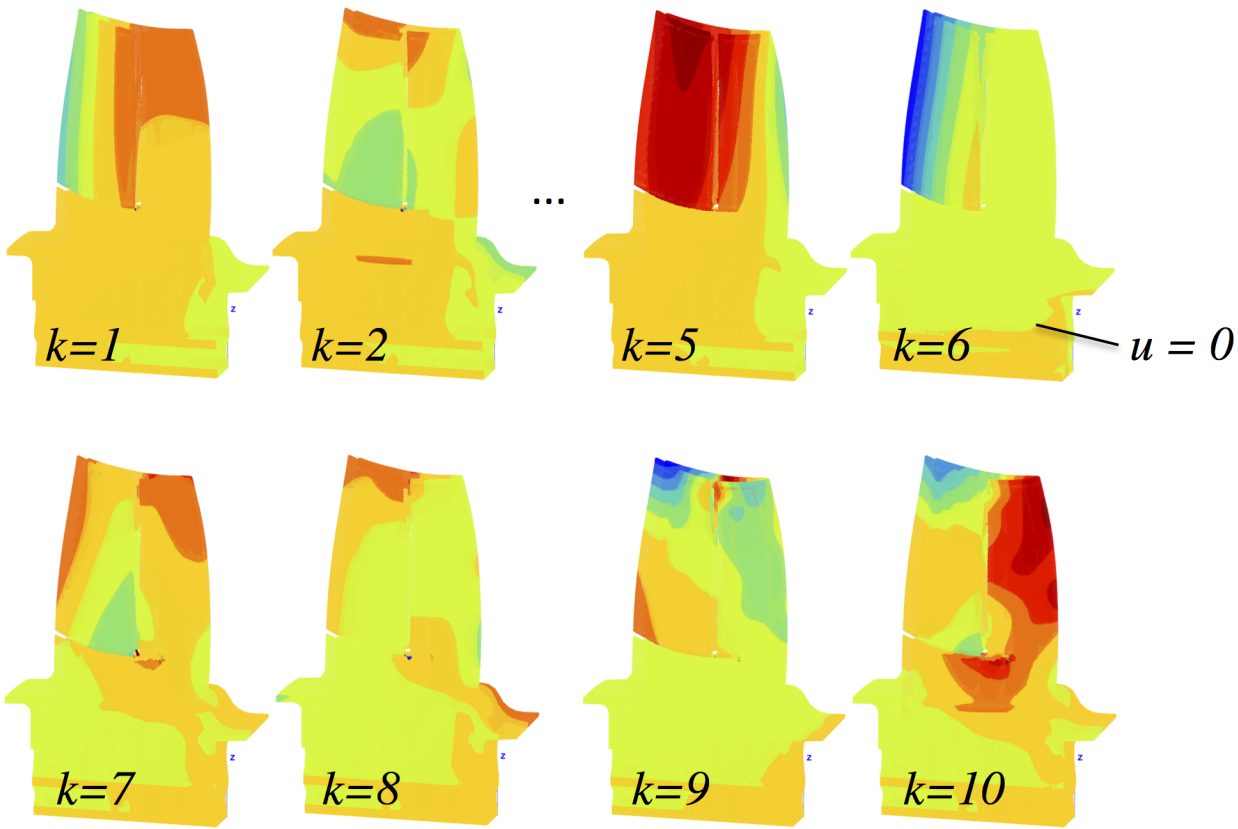

POD modes are global shape functions for model reduction.

Outline

1. Images and tensors
2. Tensor format of PDE solutions and matricization
3. Singular value decomposition (SVD)
4. PDE solution by using the finite element method
5. The setting of the Reduced equations
6. Numerical example

The usual POD Galerkin setting

$$\mathbf{u} \in \mathbf{u}^d + \mathcal{V}_h, \quad \mathcal{V}_h = \text{span}(\varphi_i)_{i=1}^{\mathcal{N}} \subset \mathcal{V}, \quad \int_\Omega \mathcal{L}(\mathbf{u})\, \mathbf{v}^*\, d\Omega = 0 \quad \forall \mathbf{v}^* \in \mathcal{V}_h$$

becomes

$$\mathbf{u} \in \mathbf{u}^d + \mathcal{V}_{ROM}, \quad \mathcal{V}_{ROM} = \text{span}(\psi_k)_{k=1}^{N} \subset \mathcal{V}_h, \quad \int_\Omega \mathcal{L}(\mathbf{u})\, \mathbf{v}^*\, d\Omega = 0 \quad \forall \mathbf{v}^* \in \mathcal{V}_{ROM}.$$

Matrix setting of the equations

Let's consider an implicite Euler scheme combined to the Newton-Raphon algorithm. We restrict our attention to a linear step of the Newton-Raphson procedure.

Matrix setting of the equations

Let's consider an implicite Euler scheme combined to the Newton-Raphon algorithm. We restrict our attention to a linear step of the Newton-Raphson procedure.

Let's $\mathbf{r}$ be the residual of the FE balance equations:

$$\mathbf{q}^{*T}\,\mathbf{r}(\mathbf{q}) = \int_\Omega \mathcal{L}(\mathbf{u})\,\mathbf{v}^*\,d\Omega, \quad \mathbf{u} = \mathbf{u}^d + \sum_i \varphi_i\,q_i, \quad \mathbf{v}^* = \sum_i \varphi_i\,q_i^*$$

The linear correction step reads:

$$\mathbf{J}(\mathbf{q})\,\delta\mathbf{q} = -\mathbf{r}(\mathbf{q}), \quad \text{avec } \mathbf{J}(\mathbf{q}) = \frac{\partial \mathbf{r}}{\partial \mathbf{q}}(\mathbf{q})$$

The new prediction of the degrees of freedom reads: $\mathbf{q} + \delta\mathbf{q}$.

Matrix setting of the equations

Let's consider an implicite Euler scheme combined to the Newton-Raphon algorithm. We restrict our attention to a linear step of the Newton-Raphson procedure.

Let's $\mathbf{r}$ be the residual of the FE balance equations:

$$\mathbf{q}^{*T}\,\mathbf{r}(\mathbf{q}) = \int_\Omega \mathcal{L}(\mathbf{u})\,\mathbf{v}^*\,d\Omega, \quad \mathbf{u} = \mathbf{u}^d + \sum_i \varphi_i\,q_i, \quad \mathbf{v}^* = \sum_i \varphi_i\,q_i^*$$

The linear correction step reads:

$$\mathbf{J}(\mathbf{q})\,\delta\mathbf{q} = -\mathbf{r}(\mathbf{q}), \quad \text{avec } \mathbf{J}(\mathbf{q}) = \frac{\partial \mathbf{r}}{\partial \mathbf{q}}(\mathbf{q})$$

The new prediction of the degrees of freedom reads: $\mathbf{q} + \delta\mathbf{q}$.

The Galerkin setting of the reduced problem reads: Find $\delta\mathbf{q} = \mathbf{V}\,\delta\boldsymbol{\gamma}$ such that,

$$\mathbf{V}^T\,\mathbf{J}(\mathbf{q})\,\mathbf{V}\,\delta\boldsymbol{\gamma} = -\mathbf{V}^T\,\mathbf{r}(\mathbf{q}), \quad \mathbf{q} = \mathbf{V}\,\boldsymbol{\gamma}.$$

Matrix setting of the equations

Let's consider an implicite Euler scheme combined to the Newton-Raphon algorithm. We restrict our attention to a linear step of the Newton-Raphson procedure.

Let's $\mathbf{r}$ be the residual of the FE balance equations:

$$\mathbf{q}^{*T}\,\mathbf{r}(\mathbf{q}) = \int_\Omega \mathcal{L}(\mathbf{u})\,\mathbf{v}^*\,d\Omega, \quad \mathbf{u} = \mathbf{u}^d + \sum_i \varphi_i\,q_i, \quad \mathbf{v}^* = \sum_i \varphi_i\,q_i^*$$

The linear correction step reads:

$$\mathbf{J}(\mathbf{q})\,\delta\mathbf{q} = -\mathbf{r}(\mathbf{q}), \quad \text{avec } \mathbf{J}(\mathbf{q}) = \frac{\partial \mathbf{r}}{\partial \mathbf{q}}(\mathbf{q})$$

The new prediction of the degrees of freedom reads: $\mathbf{q} + \delta\mathbf{q}$.

The Galerkin setting of the reduced problem reads: Find $\delta\mathbf{q} = \mathbf{V}\,\delta\boldsymbol{\gamma}$ such that,

$$\mathbf{V}^T\,\mathbf{J}(\mathbf{q})\,\mathbf{V}\,\delta\boldsymbol{\gamma} = -\mathbf{V}^T\,\mathbf{r}(\mathbf{q}), \quad \mathbf{q} = \mathbf{V}\,\boldsymbol{\gamma}.$$

It is related to the following orthogonality constrain:

$$\mathbf{J}(\mathbf{q})\,\mathbf{V}\,\delta\boldsymbol{\gamma} + \mathbf{r}(\mathbf{q}) \in \mathbb{R}^{\mathcal{N}} \quad \perp \quad \mathbf{V} \in \mathbb{R}^{\mathcal{N}\times N}$$

The computational complexity of the Galerkin procedure

$$\mathbf{V}^T\,\mathbf{J}(\mathbf{q})\,\mathbf{V}\,\delta\boldsymbol{\gamma} = -\mathbf{V}^T\,\mathbf{r}(\mathbf{q}), \quad \mathbf{q} = \mathbf{V}\,\boldsymbol{\gamma}.$$

Number of floating point operations (flops) related to $\mathbf{V}^T\,\mathbf{r}(\mathbf{q})$: $2\,N\,\mathcal{N}$.
Number of floating point operations (flops) related to $\mathbf{V}^T\,\mathbf{J}(\mathbf{q})\,\mathbf{V}$: $2\,N^2\,\mathcal{N} + 2\,N\,\mathcal{N}\,b$. Where b is the number on non-zero entries in each row of $\mathbf{J}$.

Although $N < \mathcal{N}$, the Galerkin procedure is time consuming when we need to update the tangent stiffness matrix of the ROM.

Here N must be smaller than the band width of $\mathbf{J}$ in order to reduce the computational complexity.

Outline

1. Images and tensors
2. Tensor format of PDE solutions and matricization
3. Singular value decomposition (SVD)
4. PDE solution by using the finite element method
5. The setting of the Reduced equations
6. Numerical example

Numerical simulations

Steady state thermal problem: heat conduction in a composite material. 5 parameters: thermal conductivity of each inclusion, 2 heat fluxes at the boundary ϕ_1 and ϕ_2.

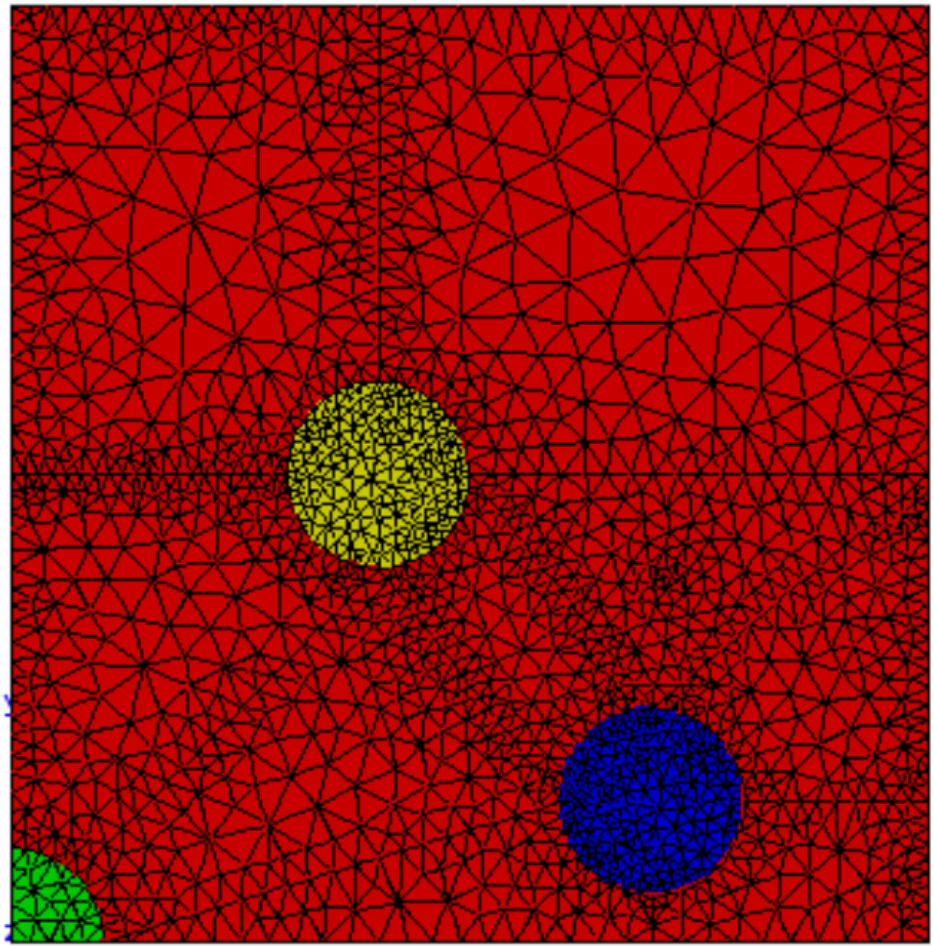

Sanpshots

Q has 7 columns.

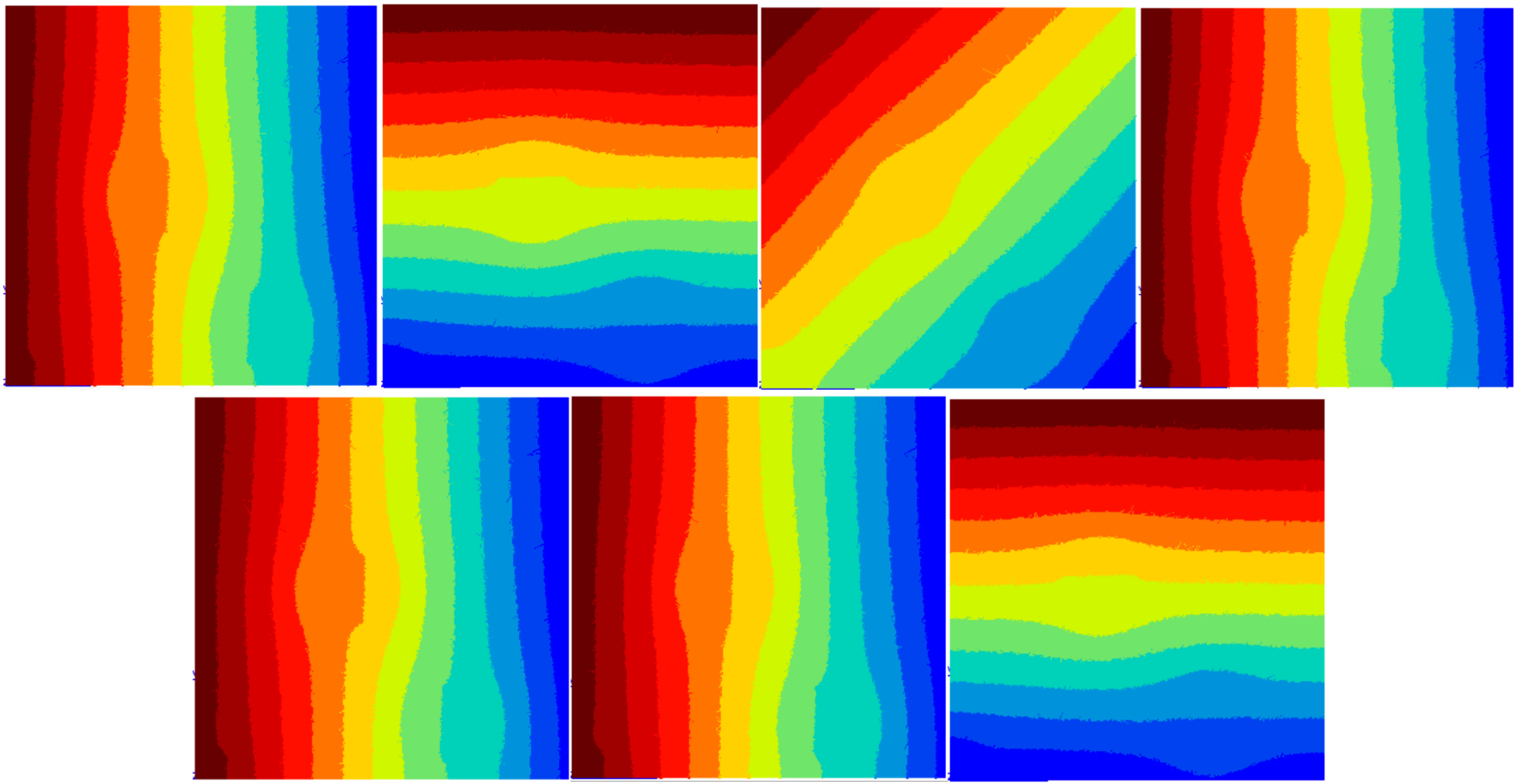

POD empirical modes

$$\mathbf{Q} = \mathbf{V}\,\mathbf{S}\,\mathbf{W}^T, \quad N = 7$$

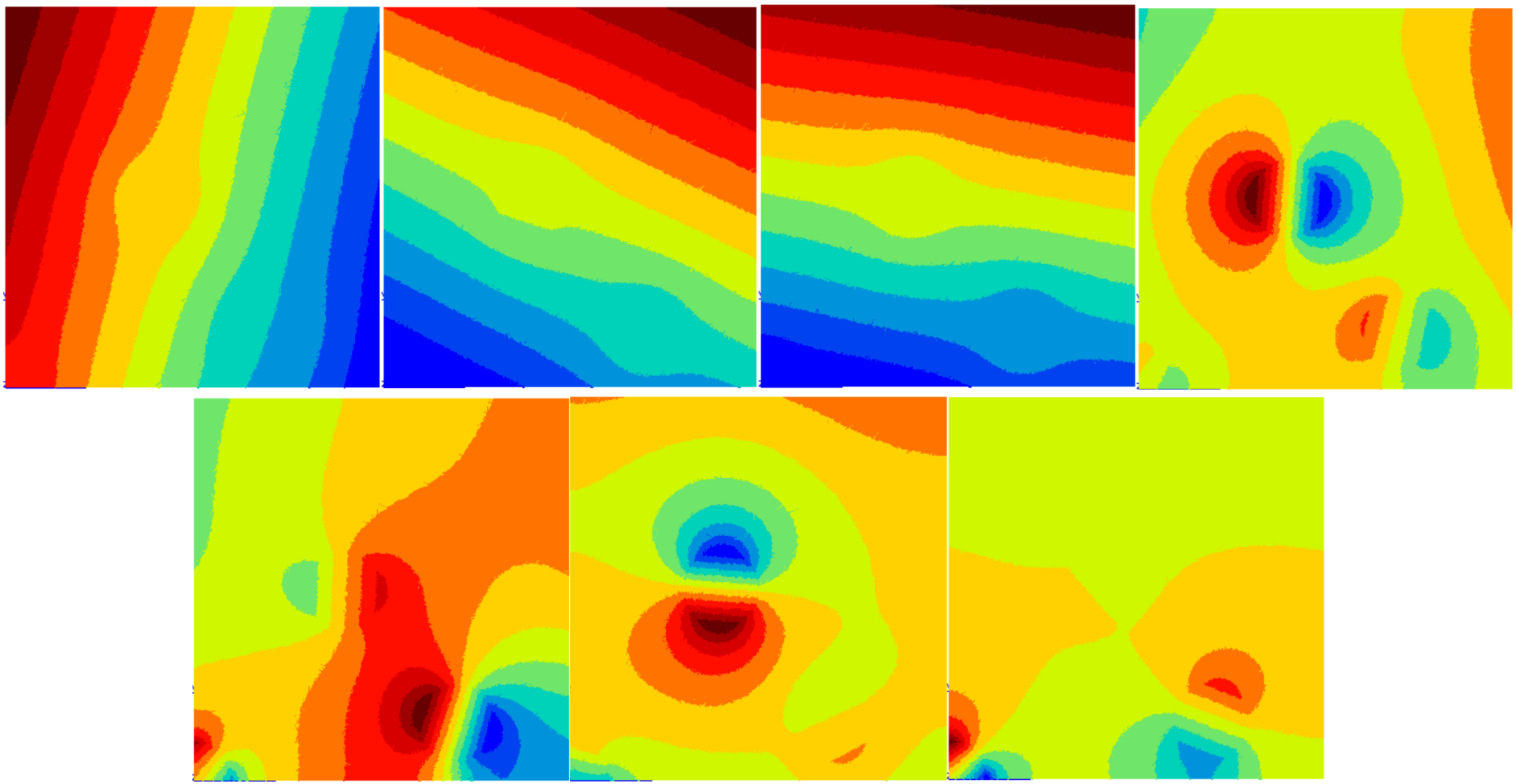

POD empirical modes

$$\mathbf{Q} = \mathbf{V}\,\mathbf{S}\,\mathbf{W}^T, \quad N = 7$$

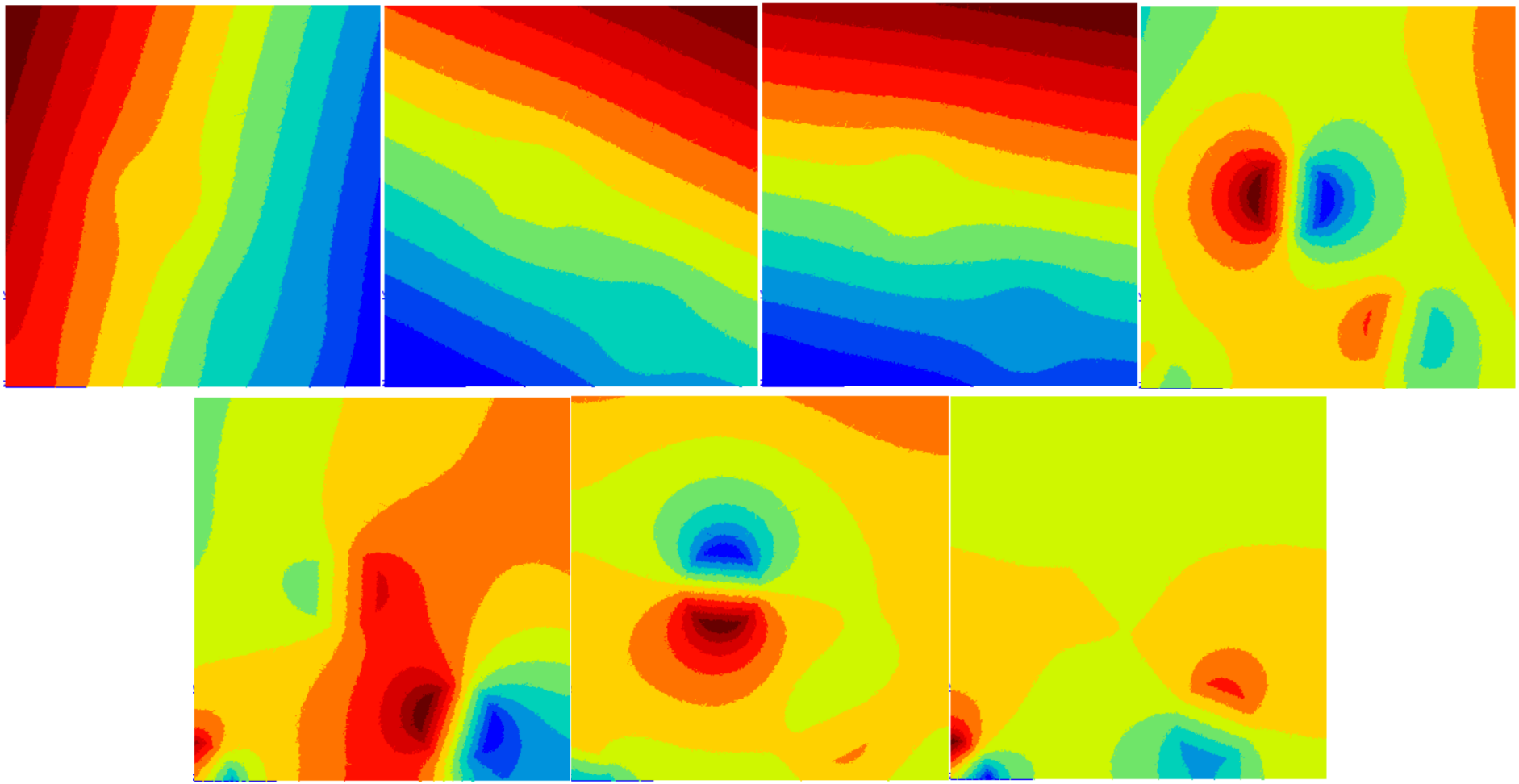

Computational time: FEM 0.3 s, Galerkin POD 0.3 s
No speedup!
50 % of the computational time is devoted to the assembly procedure.

Linear problems with affine parameter dependence

Here

$$\mathbf{J}(\boldsymbol{\mu}) = \mathbf{J}_o + \mu_1\,\mathbf{J}_1 + \mu_2\,\mathbf{J}_2 + \mu_3\,\mathbf{J}_3$$

$$\mathbf{r}(\boldsymbol{\mu}) = \mu_4\,\mathbf{r}_4 + \mu_5\,\mathbf{r}_5$$

Then, the following projections can be performed during the offline phase:

$$\mathbf{J}_i^R = \mathbf{V}^T\,\mathbf{J}_i\,\mathbf{V}, \quad i = 0, 1, 2, 3$$

$$\mathbf{r}_i^R = \mathbf{V}^T\,\mathbf{r}_i\,\mathbf{V}, \quad i = 4, 5$$

The online operations reads:

$$(\mathbf{J}_0^R + \mu_1\,\mathbf{J}_1^R + \mu_2\,\mathbf{J}_2^R + \mu_3\,\mathbf{J}_3^R)\,\boldsymbol{\gamma} = \mu_5\,\mathbf{r}_4^R + \mu_5\,\mathbf{r}_5^R$$

But the extension of this decomposition in not straightforward for nonlinear problems involving threshold effects. Solutions are proposed by the Empirical Interpolation Method or Hyper-reduction methods.

Outlook

In the future,

- less data destruction
- more massive experimental data (Tomography, ...)
- more image processing
- more parameters in numerical models
- more FE simulations and more simulation data
- high dimensional visualizations and collaborative tools
- more model reduction and data compression
- hybrid Full-order/reduced-order modeling (Partial far field mechanics)